Time-Dependent Semiclassical Theory of Gain-Coupled Distributed Feedback Lasers

IRL N. DULING III AND M. G. RAYMER

Abstract—A semiclassical treatment of the time-dependent behavior of a gain-coupled, distributed feedback laser (DFL) has been developed. This treatment takes into account the field propagation within the DFL, and is therefore capable of predicting its behavior even for extremely short pump pulses. Comparisons are made to existing steady-state and transient theories where they are valid, showing good agreement, and new predictions are made of the behavior in the short pump pulse regime. It is found that the emitted pulse duration is dominated by the transit time through the pumped region. By studying the evolution of the field distribution inside the cavity, insight can be gained into the operation of the DFL. The effect of spatial hole burning in a gain-coupled DFL is treated and found to be small.

I. Introduction

RECENT interest in the transient behavior of distributed feedback lasers has led to the need for a more complete theoretical analysis than has existed previously. The photon rate equation model used by Bor [1] treats the time dependence of the laser output, but due to the mean field approximation inherent in this theory it is unable to treat the regime where spatial propagation and cavity length become important in determining the output pulse duration. This regime is of particular interest because of the possibility of producing single pulses of picosecond duration from such lasers.

The fundamental characteristic of a distributed feedback laser (DFL) is that in the absence of external mirrors, the necessary feedback is provided by Bragg scattering from spatially periodic variations of the complex refractive index of the laser medium. This can be either the real component or imaginary component (gain) of the material index or the effective index (as in an optical waveguide). In the case where the gain is used to vary the complex index a nonlinear coupling occurs between the gain and the optical field. As the light intensity in the excited region increases, the gain is depleted, destroying the feedback and allowing the light to escape the medium. This self cavity dumping can, for a range of pump energies, produce a train of ultrashort pulses. Typically these pulses are 50–100 times shorter than the pump pulse used [2].

Manuscript received January 19, 1984; revised May 29, 1984. This work was supported in part by the Empire State Electric Energy Research Corporation, General Electric Company, the New York State Energy Research and Development Authority, Northeast Utilities, the Standard Oil Company (Ohio), and the University of Rochester. Such support does not imply endorsement of the content by any of the above parties.

I. N. Duling III is with the Laboratory for Laser Energetics and the Institute of Optics, University of Rochester, Rochester, NY 14623.

M. G. Raymer is with the Institute of Optics, University of Rochester, Rochester, NY 14627.

In order to model this transient regime more completely, a semiclassical theory is developed which incorporates both the temporal and spatial variations of the field and population inversion within the laser cavity. As in the existing steady-state analyses [3], [4] the laser field is modeled as two counter-propagating waves coupled by Bragg reflection. The derivation of the basic equations is presented in Section III. Section II is a brief review of the previous rate equation model given for comparison. Section IV presents comparisons of the new theory to the existing steady state and transient theories in the appropriate limits. Further predictions in the region where the previous transient theory is not valid are also included. An analysis of the effect of spatial hole burning is presented in the Appendix.

II. Photon Rate Equation Model

The photon rate equation model analyzed by Bor [1] treats the medium shown in Fig. 1 as a four-level system where $2 \rightarrow 1$ is the lasing transition. Here, σ_a and σ_e are the absorption and emission cross sections, λ_2 is the pump rate into level 3, the γ's are spontaneous or nonradiative rates (γ_{10} and γ_{32} are assumed large), and ω_0 is the atomic frequency of the $2 \rightarrow 1$ transition. The rate equations with $W \equiv$ population inversion density and $q \equiv$ photon density are

$$\dot{W} = \lambda_2(N - W) - \frac{\sigma_e c}{n} W q - \gamma_{21} W \tag{1}$$

$$\dot{q} = \frac{\sigma_e c}{n} W q - \frac{q}{\tau_c} + \Omega \gamma_{21} W \tag{2}$$

where

$$\tau_c = \frac{nL^3}{8c\pi^2} (W\sigma_e V)^2$$

is the effective cavity decay time

$L \equiv$ length of the excited region

$V \equiv$ visibility of the gain modulation

$n \equiv$ refractive index of the host material

$$\Omega = \frac{b}{N\sigma_a L^2 S}$$

is the fraction of spontaneous emission contributing to the laser output

$b \equiv$ vertical focus parameter

0018-9197/84/1000-1202$01.00

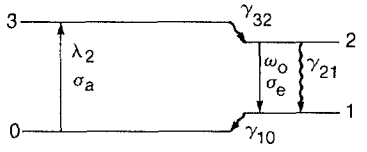

Fig. 1. The four level system used for both the photon and semiclassical rate equations. The decay rates 32 and 10 are assumed large.

$N \equiv$ lasing species density

$S \equiv$ spectral fraction of contributing spontaneous emission.

Throughout this paper a dot, e.g., $\dot{W}$, indicates a partial derivative with respect to time.

This theory correctly predicts the transient behavior of the gain-coupled distributed feedback laser in the limit where the pump duration (T_p) is much longer than the transit time of the laser light along the pumped region (nL/c). When $T_p \leqslant nL/c$ the spatially varying field distribution must be considered in order to determine the output pulse characteristics. Since the photon rate equation model considers only the photon number in the cavity (mean field approximation) it is unable to accurately predict the DFL output characteristics in this regime. Results of this model for laser output pulse duration are compared in Section V with those from the semiclassical theory presented here.

III. Semiclassical Theory of the DFL

A. Population Equations

As in the rate equation theory, the gain medium is modeled according to Fig. 1. Following the approach of Sargent *et al.*, [4] the system is described by the equations for the density matrix

$$\dot{\rho}_{11} = -\gamma_{10}\rho_{11} + \gamma_{21}\rho_{22} + \left(\frac{i}{\hbar} V_{21}\rho_{12} + \text{c.c.}\right) \tag{3a}$$

$$\dot{\rho}_{22} = \lambda_2 - \gamma_{21}\rho_{22} - \left(\frac{i}{\hbar} V_{21}\rho_{12} + \text{c.c.}\right) \tag{3b}$$

$$\dot{\rho}_{21} = -(i\omega_0 + \gamma)\rho_{21} + \frac{i}{\hbar} V_{21}(\rho_{22} - \rho_{11}). \tag{3c}$$

Note that ρ_{ii} is the population of level i and γ is the homogeneous linewidth of the lasing transition. $V_{21} = -pE(z, t)$ is the atomic interaction energy, p is the dipole matrix element, $E(z, t) = \frac{1}{2}(A(z, t) \exp(i\omega t) + \text{c.c.})$ is the electric field in terms of the slowly varying envelope $A(z, t)$. Here c.c. denotes the complex conjugate.

The density matrix equations can be simplified by making the rate equation approximation for the gain medium (not the fields), which is valid when the linewidth γ is sufficiently large [4], [5]. After formally integrating (3c) and assuming that $A(z, t)$ and the population inversion $w(z, t) \equiv \rho_{22} - \rho_{11}$ vary little in time γ^{-1}, ρ_{21} becomes approximately

$$\rho_{21} = \frac{-ip}{2\hbar} \frac{A^* w}{i\Delta + \gamma} e^{-i\omega t} \tag{4}$$

where $\Delta = \omega_0 - \omega$ and nonresonant terms have been neglected (rotating wave approximation [6]). Substituting (4) into (3a) and (3b) leads to

$$\dot{\rho}_{22} = \lambda_2 - \gamma_{21}\rho_{22} - \frac{p^2}{2\hbar^2} \frac{\gamma}{\Delta^2 + \gamma^2} |A|^2 w \tag{5a}$$

$$\dot{\rho}_{11} = \gamma_{21}\rho_{22} - \gamma_{10}\rho_{11} + \frac{p^2}{2\hbar^2} \frac{\gamma}{\Delta^2 + \gamma^2} |A|^2 w. \tag{5b}$$

The equations are further simplified by assuming that γ_{10} is large so that $\rho_{11} << \rho_{22}$ and $w \simeq \rho_{22}$. Then the inversion w obeys

$$\dot{w} = \lambda_2 - \gamma_{21} w - B|A|^2 w \tag{6}$$

where

$$B = \frac{p^2}{2\hbar} \left(\frac{\gamma}{\Delta^2 + \gamma^2}\right).$$

To provide feedback for the gain-coupled DFL the pumping rate λ_2 is spatially modulated with a period $\Lambda = \pi/\beta_0$,

$$\lambda_2 = N\lambda(t)(1 + V \cos 2\beta_0 z) \tag{7}$$

where, again, V is the visibility of the fringes and where $\lambda(t)$ accounts for the time dependence of the pumping, which may be provided by a laser pulse. To remove the rapid spatial modulation from the equations, and to go to a macroscopic description, a new inversion density variable W is defined by

$$W = \frac{Nw}{1 + V \cos 2\beta_0 z}. \tag{8}$$

The equation for the time dependence of W is then, from (6),

$$\dot{W} = N\lambda - \gamma_{21} W - B|A|^2 W. \tag{9}$$

B. Field Equations

The field evolution is determined by the wave equation

$$\left[\frac{\partial^2}{\partial z^2} - \frac{n^2}{c^2}\frac{\partial^2}{\partial t^2}\right] E(z, t) = \frac{4\pi n^2}{c^2} \frac{\partial^2}{\partial t^2} \mathcal{P}(z, t) \tag{10}$$

where the polarization $\mathcal{P} = \frac{1}{2}[P(z, t) \exp(i\omega t) + \text{c.c}]$.

If $A(z, t)$ is separated into two counter-propagating waves

$$A(z, t) = \text{Re}^{i\beta_0 z} + \text{Se}^{-i\beta_0 z} \tag{11}$$

and substituted into (10) we obtain (ignoring second derivatives of R and S as well as the first derivative of P)

$$\left[i\beta_0 R' - \frac{1}{2}\left(\beta_0^2 - \frac{\omega^2 n^2}{c^2}\right) R - \frac{i\omega n^2}{c^2}\dot{R}\right] e^{+i\beta_0 z} - \left[-i\beta_0 S' + \frac{1}{2}\left(\beta_0^2 - \frac{\omega^2 n^2}{c^2}\right) S + \frac{i\omega n^2}{c^2}\dot{S}\right] \cdot e^{-i\beta_0 z} = \frac{2\pi n^2 \omega^2}{c^2} P \tag{12}$$

where a prime (e.g., R') indicates a partial derivative with respect to z. In the semiclassical theory the polarization is determined by

$$P = 2Np\rho_{12} e^{-i\omega_0 t}. \tag{13}$$

Using the value of $\rho_{12} = \rho_{21}^*$ from (4) we get

$$P = -\frac{iNp^2}{\hbar}\frac{Aw}{i\Delta+\gamma}. \tag{14}$$

Significant feedback occurs only for $\beta \simeq \beta_0$. Using this fact and (14), (12) can be separated into the following two equations

$$R' - \frac{n}{c}\dot{R} + (\alpha W - i\delta)R = -\frac{\alpha VW}{2}S \tag{15a}$$

$$-S' - \frac{n}{c}\dot{S} + (\alpha W - i\delta)S = -\frac{\alpha VW}{2}R \tag{15b}$$

where $\delta = (\beta^2 - \beta_0^2)/2\beta_0$ and $\alpha = -2\pi\beta Np^2/\hbar(i\Delta+\gamma)$. Equation (15) was obtained by neglecting terms in $\exp(\pm i3\beta_0 z)$, i.e., assuming that W is slowly varying spatially. This neglects spatial hole burning, which is treated in the Appendix, and is found to be relatively unimportant, in agreement with the steady-state case [4].

Depletion of the ground state, level 0, is accounted for in the normal manner through the pump term $\lambda(t)$, i.e., by replacing

$$\lambda N \rightarrow \lambda(N - W). \tag{16}$$

In order to simulate spontaneous emission, a uniform noise term equivalent to one photon in the excited region was introduced into the field equations. The time averaged energy

$$\overline{\int_{V_0} \frac{E_0^2}{4\pi}\, dV} = \hbar\omega_0$$

where the integral is over the volume V_0 of the excited region. Assuming the noise to be equal in both directions, we find for the noise fields

$$R_0 = S_0 = \sqrt{\frac{4\pi\hbar\omega_0}{V_0}}. \tag{17}$$

The final equations are then,

$$R' - \frac{n}{c}\dot{R} + (\alpha W - i\delta)(R + R_0) = -\frac{\alpha WV}{2}S \tag{18a}$$

$$-S' - \frac{n}{c}\dot{S} + (\alpha W - i\delta)(S + S_0) = -\frac{\alpha WV}{2}R \tag{18b}$$

$$\dot{W} = \lambda(N - W) - \gamma_{21}W - B(|R|^2 + |S|^2)W. \tag{18c}$$

In going from (9) to (18c) the cross terms of $|A|^2$ were neglected, consistent with the assumption of no spatial hole burning (see the Appendix).

IV. Theoretical Predictions

Equation (18) was solved numerically. Due to the counterpropagating nature of the field solutions, a second order Euler method was used which required a square integration grid ($\Delta z = c\Delta t$). The equation was integrated subject to the boundary conditions $S(L, t) = R(0, t) = W(z, 0) = 0$, and $\lambda(t)$ is Gaussian in time and uniform in space.

The system parameters where chosen appropriate for Rodamine 6G in ethylene glycol as the active medium in the distributed feedback laser, i.e., $N = 3.5 \times 10^{-3} \cdot M$ (2.1×10^{18} molecules/cm^2), $V_0 = bL/N\sigma_a$, $b = 0.025$ cm, $\sigma_a = 2.7 \times 10^{-16}$ cm^2, $\alpha = \sigma_e/2, \sigma_e = 1.4 \times 10^{-16}$ cm^2, $\tau = 1/\gamma_{21} = 4$ ns, $V = 1.0$, $n = 1.44$.

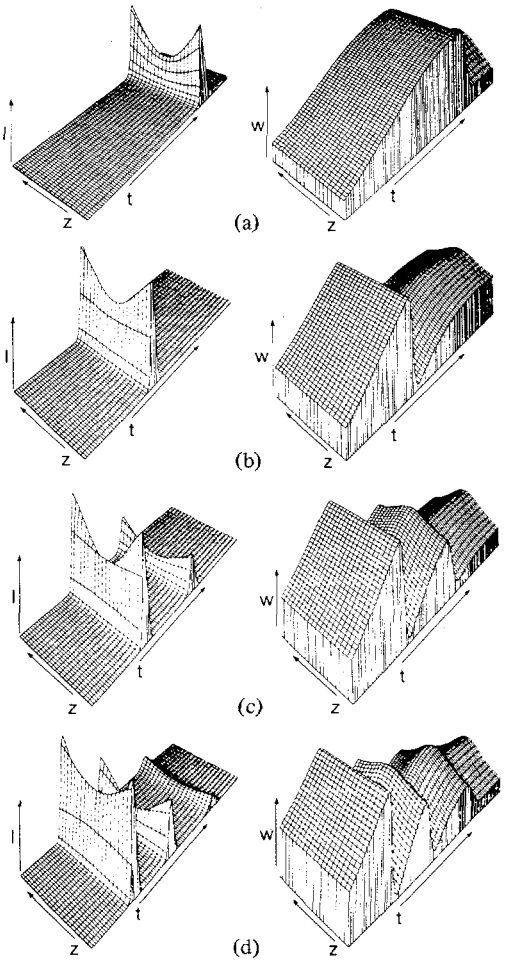

Fig. 2. Total intensity $I = R^2 + S^2$ and population inversion density W plotted as functions of time and space for an increasing pump energy. The pump pulse duration was 70 ps, and the pumped region was 0.1 cm in length. The relative values of the pump energies are (a) 0.5, (b) 1.1, (c) 1.5, and (d) 2.0. The vertical scales are normalized and the time axis represents 120 ps full scale.

Due to the nonlinear coupling between the gain, the Bragg reflectivity, and the field, a self cavity-dumping is observed for a range of pump energies in the DFL. The inversion builds up as the integral of the pump pulse until the field increases sufficiently for gain saturation to become dominant. At this time, the Bragg reflectivity decreases rapidly allowing the field to escape as a pulse. If this process occurs during the pump pulse the inversion has the opportunity to recover and produce a second pulse. As the pump energy is increased, the initial dumping will occur at earlier times allowing additional pulses to be produced. In Fig. 2, the total intensity $I = R^2 + S^2$, and population inversion W are shown for a sequence of pump energies. The solutions are plotted as functions of space and time. The laser output is directly proportional to the value of the total intensity at the end face ($z = 0, L$) of the pumped region. The behavior of these solutions at the end faces is in excellent qualitative agreement with the photon rate equation model [1].

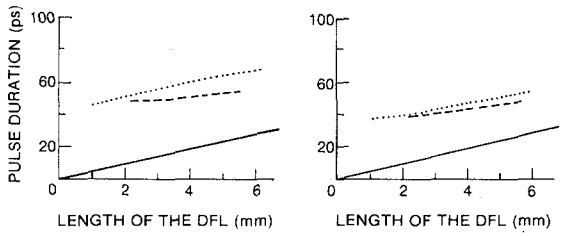

Fig. 3. Duration of the first pulse as a function of the length of the DFL for a 3.5 ns pump pulse and (a) the second pulse at threshold, (b) the third pulse at threshold. The dashed line corresponds to the photon rate equation prediction, and the dotted line to the semiclassical prediction. The solid line is $t = nL/c$.

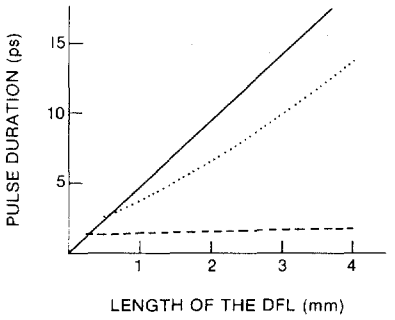

Fig. 4. Duration of the first pulse as a function of the length of the DFL for a 70 ps pump pulse and the second pulse at threshold. The dashed line is that predicted by the photon rate equation model and the dotted line is that predicted by the semiclassical theory. The solid line is $t = nL/c$.

Using the previously published predictions [7] of the photon rate equations for the duration of the initial output pulse as a function of the length of the pumped region given that either a) the second pulse is at threshold or b) the third pulse is at threshold, the new theory can be quantitatively evaluated as to its performance in the limit of long pump pulses, $T_p >> nL/c$. This comparison is shown in Fig. 3 for a pump pulse of 3.5 ns. The results show excellent agreement between the two theories in this limit. It is interesting to note that, although there is an offset, the slope of the dependence is very close to that of the line $t = nL/c$.

It has been shown previously that as the pump pulse width is reduced, the pulse duration of the DFL will also shorten [2]. However, as the pump pulse duration becomes comparable to the pumped region transit time ($T_p = nL/c$) the photon rate equation analysis will be invalid. In Fig. 4, the predicted pulse width versus pumped region length [similar to Fig. 3(a)] in the case of a 70 ps pump pulse is shown for the two theories. Again, the line $t = nL/c$ is shown. A large discrepancy between the theories is evident which, as expected, decreases as the length of the pumped region is decreased. It is seen that the pulse widths are much longer than predicted by the photon rate equations and that their duration approaches the transit time nL/c.

In the steady-state limit, $\dot{S} = \dot{R} = 0$, the field equations (15) reduce directly to the form of previous steady-state theories [3], [4] in the gain-coupled case. The amount of Bragg reflectivity at any point is proportional to the coefficient of the coupling term in the field equations. The value of this coupling

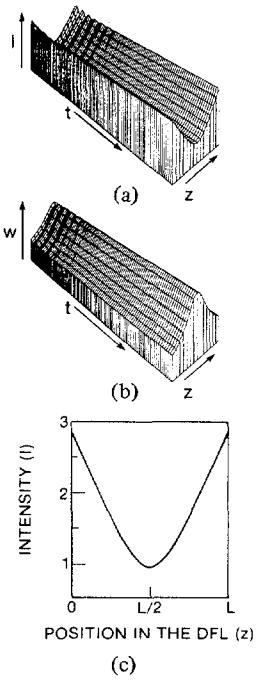

Fig. 5. The intensity I and inversion density W as functions of space and time for steady-state pumping, (a) and (b), and the final intensity distribution along the length of the DFL, (c). The length of the DFL was 0.3 cm, and the time axis is 120 ps full scale.

coefficient determines the nature of the field distribution. For a gain-coupled laser, the coupling coefficient can be expressed as $\alpha VWL/2$. It has been shown in the steady-state analyses that if $\alpha VWL/2 < 1.5$, termed undercoupled, the field distribution will be peaked toward the ends of the pumped region, while if $\alpha VWL/2 > 1.5$, termed overcoupled, the distribution will be peaked in the center of the cavity. In the case of steady-state pumping shown in Fig. 5, after the initial oscillations damp out, the coupling coefficient can be calculated for different positions in the pumped region. The coupling coefficient varies from 0.42 at the edge of the region ($z = 0, L$) to 1.3 in the center ($z = L/2$) where it is a maximum. This evaluation agrees with the form of the intensity distribution seen in Fig. 5(c), which shows behavior typical of undercoupling.

We have found that due to gain saturation in a laser of this type, the high values of αVWL required for overcoupled operation cannot be maintained in the steady state. However, during the transient field build-up, prior to gain saturation, the coupling coefficient can reach values in the overcoupled range. This results from the gain overshooting the steady-state value prior to the field build-up. As the field builds up it experiences strong coupling and therefore peaks in the center of the cavity. Then, as the transient field depletes the gain, the laser shifts to the undercoupled regime enabling the pulse to escape. In Fig. 6, three-dimensional plots of two cases are shown. For each case the plot is viewed both from earlier times, Fig. 6(a) and (c), and from later times Fig. 6 (b) and (d) to allow examination of the intensity distribution as it evolves. In Fig. 6(a) the contours of equal time can be seen to have positive curvature indicating an overcoupled intensity distribution, while at later times, Fig. 6(b), the contours show the negative curvature typical of undercoupled operation. Fig. 6(c) and (d)

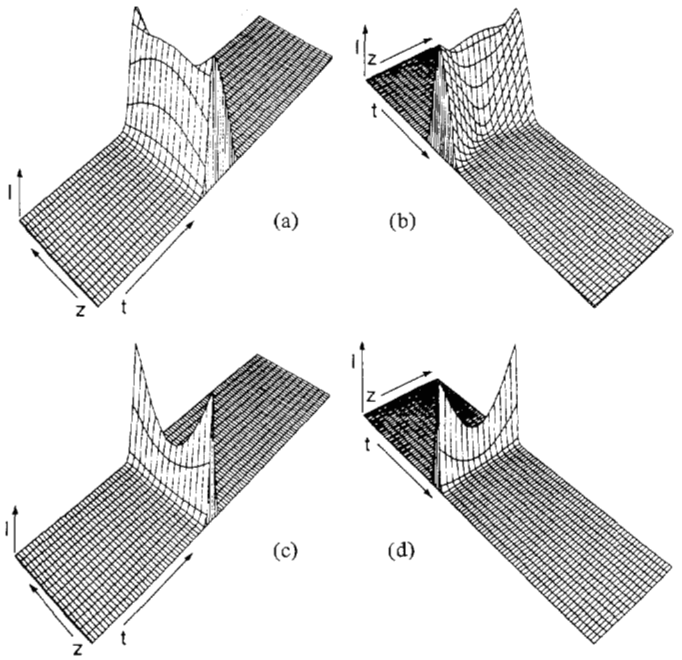

Fig. 6. The intensity as functions of space and time for the case of the DFL of length 0.3 cm, (a) and (b), and 0.03 cm, (c) and (d). In both cases the pump intensity was adjusted so that the second pulse was at threshold. For each case the intensity distribution is shown as seen from earlier times, (a) and (c), or from later times (b) and (d). The full scale time is 120 ps.

are the same views of the field when the pumped region is made shorter. In this case the operation is undercoupled ($\alpha VWL/2 < 1.5$) even during the build up, as seen by negative curvatures at all times.

V. Conclusion

Due to the inability of the photon rate equation analysis of the DFL to predict the output characteristics accurately in the regime where the pumped-region transit time is comparable to the pump pulse length, a semiclassical treatment has been developed which takes into account the spatial variation of the field and inversion along the pumped region. The addition of this consideration provides a theory capable of handling both the short-time transient regime and the steady-state theories Comparisons with existing transient and steady-state theories show good agreement in the limits where those theories are valid, and predictions are made in the short-pulse regime where the photon rate equation is invalid. These predictions indicate that the pulse duration is dominated by the transit time along the pumped region. Also, a careful evaluation of the field evolution shows that in some cases the laser is overcoupled at early times and, as the pulse is emitted, becomes undercoupled, while in other cases the operation remains undercoupled throughout the build-up and pulse emission process. This provides new insight into the mechanisms involved in the DFL. Further refinements of this theory which may have an effect on the output characteristics are to include excited state absorption, reabsorption of the lasing light in the case of dye lasers, molecular rotation and diffusion, and the addition of a saturable absorber to the medium.

Appendix

Spatial Hole Burning

Omission of the exp ($\pm i3\beta_0 z$) terms in (15) and the cross-terms of $|A|^2$ in (18c) is equivalent to ignoring spatial hole burning, whose effect in a DFL is to flatten the peaks of the gain modulation. A fairly straightfoward analysis can be made by factoring an additional modulation term out of the inversion W. In addition to (7) and (8) then, we define

$$W = W_0 + W_1 \cos(2\beta_0 z + \psi) \tag{A1}$$

where the coefficients are obtained as in Fourier analysis,

$$W_0 = \frac{1}{\Lambda} \int_{\Lambda} W dz \quad \text{(integral over one grating period)} \tag{A2a}$$

$$W_1 \simeq 2\frac{1}{\Lambda} \int_{\Lambda} W \cos(2\beta_0 z + \psi) dz. \tag{A2b}$$

W_0 is thus the local average of the inversion, and W_1 describes the strength of spatial hole burning. We take the phase to be that which leads to maximum gain, $\psi = 0$, determined by requiring maximum spatial overlap of the intensity distribution with the gain distribution. The equations governing the population inversion are obtained by differentiating (A2) with respect to time and substituting for $\dot{W}$ from (9). After integrating over one grating spacing we find

$$\dot{W}_0 = \lambda - \gamma_{21} W_0 - B(|R|^2 + |S|^2) W_0 - B|RS| W_1 \tag{A3a}$$

$$\dot{W}_1 = -\gamma_{21} W_1 - B(|R|^2 + |S|^2) W_1 - 2B|RS| W_0. \tag{A3b}$$

Starting from (12) and (14) and using (A1), the field equations become

$$R' - \frac{n}{c}\dot{R} + \alpha W_0 R - i\delta R = -\frac{\alpha V}{2} W_0 S - \frac{\alpha V}{2} W_1 R - \frac{\alpha}{2} W_1 S \tag{A4a}$$

$$-S' - \frac{n}{c}\dot{S} + \alpha W_0 S - i\Delta S = -\frac{\alpha V}{2} W_0 R - \frac{\alpha V}{2} W_1 S - \frac{\alpha}{2} W_1 R. \tag{A4b}$$

To obtain these equations, we neglected terms of the form exp ($\pm i5\omega_0 z$). This iterative procedure could be extended to higher harmonics of ω_0 if desired.

When these modifications were included in the numerical solution, it was found that it had little or no effect on the output fields. A typical case is shown in Fig. 7. The holeburning strength W_1 peaks in the center of the pumped region ($z = L/2$) as seen in Fig. 7(c). This is expected since its source term depends on the product of the fields $|RS|$, and one of these fields is always zero at the ends of the region. If the magnitude of the holeburning strength W_1 is compared to the average inversion W_0 at the center of the pumped region, it is found that W_1 grows to 0.36 W_0 for this case. This appears to be in-

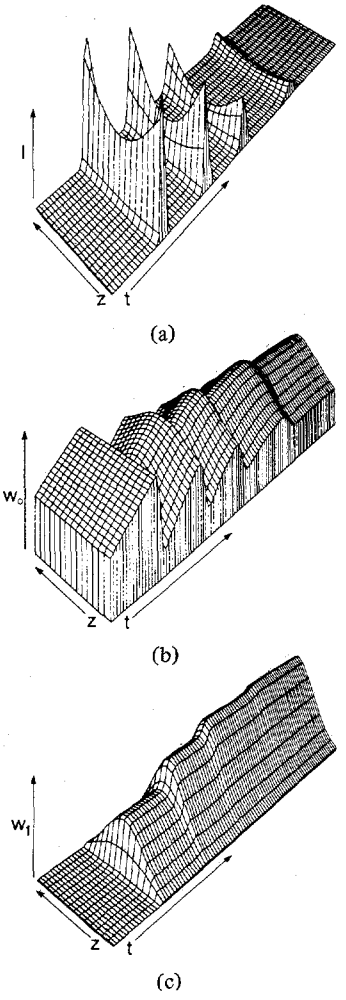

Fig. 7. Plotted as function of space and time are (a) the intensity, I, (b) the local average inversion W_0, and (c) the negative of the hole-burning strength $-W_1$. The length of the DFL was 0.03 cm, and a 70 ps pump pulse was used. The full scale time is 120 ps.

sufficient to significantly alter the laser output. The only observable change is a decrease (12 percent) in the peak output power and a slight increase (4 percent) in the time between pulses. This increase is probably due to a higher lasing threshold as a result of the descreased fringe visibility. The negligible effect of spatial hole burning is consistent with the findings of Sargent *et al.*, [4] in the steady-state analysis of the gain-coupled distributed feedback laser.

References

[1] Zs. Bor, "Tunable picosecond pulse generation by an N_2 laser pumped self Q-switched distributed feedback dye laser," *IEEE J. Quantum Electron.*, vol. QE-16, pp. 517-524, 1980.
[2] G. Szabo, Zs. Bor, and A. Muller, "Amplification and measurement of single 1.6-3.5 ps pulses generated by a distributed feedback dye laser," *Appl. Phys.*, vol. B-31, pp. 1-4, 1983.
[3] H. Kogelnik and C. V. Shank, "Coupled-wave theory of distributed feedback lasers," *J. Appl. Phys.*, vol. 43, pp. 2327-2335, 1972.
[4] M. Sargent, W. H. Swatner, and J. D. Thomas, "Theory of a distributed feedback laser," *IEEE J. Quantum Electron.*, vol. QE-16, pp. 465-472, 1980.
[5] L. Allen and J. H. Eberly, *Optical Resonance and Two Level Atoms.* New York: Wiley, 1975, p. 134.
[6] —, *Optical Resonance and Two Level Atoms.* New York: Wiley, 1975, p. 28.
[7] Zs. Bor, A. Muller, B. Racz, and F. P. Schäfer, "Ultrashort pulse generation by distribution feedback dye lasers I," *Appl. Phys. B.*, vol. 27, pp. 9-14, 1982.

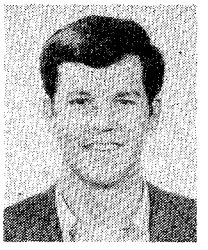

Irl N. Duling III was born in Wilmington, DE, on November 28, 1956. He received the B.Sc. degree in physics from the Massachusetts Institute of Technology, Cambridge, in 1978. He is presently working towards the Ph.D. degree with a concentration in transient phenomena in distributed feedback lasers at the University of Rochester, Rochester, NY.

Between June 1978 and August 1979 he was employed by the Raytheon Corporation, Wayland MA, in their Electro-Optics Department, working on CO_2 laser based Doppler imaging systems.

Mr. Duling is a member of the Optical Society of America.

M. G. Raymer, photograph and biography not available at the time of publication.